AFRL-RY-WP-TP-2007-111

TRANSFORMATIONAL ELEMENT LEVEL ARRAYS (TELA) TESTBED (Preprint)

Thomas Dalrymple, Jonathan Buck, Peter Buxa, John McCann, Robert Neidhard, Gary Scalzi, Caleb Shreffler, Dan Spendley, and Paul Watson

RF/EO Subsystems Branch
Aerospace Components and Subsystems Division

SEPTEMBER 2007

AIR FORCE RESEARCH LABORATORY
SENSORS DIRECTORATE
WRIGHT-PATTERSON AIR FORCE BASE, OH 45433-7320
AIR FORCE MATERIEL COMMAND
UNITED STATES AIR FORCE

REPORT DOCUMENTATION PAGE

Form Approved
OMB No. 0704-0188

1. REPORT DATE *(DD-MM-YY)*	2. REPORT TYPE	3. DATES COVERED *(From - To)*
September 2007	Conference Paper Preprint	01 June 2007 – 15 August 2007

4. TITLE AND SUBTITLE

TRANSFORMATIONAL ELEMENT LEVEL ARRAYS (TELA) TESTBED (Preprint)

5a. CONTRACT NUMBER
IN-HOUSE

5b. GRANT NUMBER

5c. PROGRAM ELEMENT NUMBER
62204F

6. AUTHOR(S)

Thomas Dalrymple, Jonathan Buck, Peter Buxa, John McCann, Robert Neidhard, Gary Scalzi, Caleb Shreffler, Dan Spendley, and Paul Watson

5d. PROJECT NUMBER
7622

5e. TASK NUMBER
11

5f. WORK UNIT NUMBER
7622110K

7. PERFORMING ORGANIZATION NAME(S) AND ADDRESS(ES)

RF/EO Subsystems Branch
Aerospace Components and Subsystems Division
Sensors Directorate
Air Force Research Laboratory
Wright-Patterson Air Force Base, OH 45433-7320

8. PERFORMING ORGANIZATION REPORT NUMBER
AFRL-RY-WP-TP-2007-111

9. SPONSORING/MONITORING AGENCY NAME(S) AND ADDRESS(ES)

Air Force Research Laboratory
Sensors Directorate
Wright-Patterson Air Force Base, OH 45433-7320
Air Force Materiel Command
United States Air Force

10. SPONSORING/MONITORING AGENCY ACRONYM(S)
AFRL/RYDR

11. SPONSORING/MONITORING AGENCY REPORT NUMBER(S)
AFRL-RY-WP-TP-2007-111

12. DISTRIBUTION/AVAILABILITY STATEMENT
Approved for public release; distribution unlimited.

13. SUPPLEMENTARY NOTES
Paper contains color. This is a work of the U.S. Government and is not subject to copyright protection in the United States. PAO case number AFRL/WS 07-1892, 14 August 2007. Submitted for publication in the Allerton Antenna Applications Symposium Digest, Urbana-Champaign, IL, 26 September 2007.

14. ABSTRACT

The Air Force is in need of antenna technologies to support surveillance needs in a complex Radio Frequency (RF) environment. Requirements dictate the need to find weak and strong emitters simultaneously over broad bandwidth, while resolving emitter data such as angle of arrival and time of arrival for signal identification and tracking.

Previous work at AFRL has resulted in many technologies that support these needs. Many components exist today that were only theoretical a few years ago, such as phased array antennas that support 10:1 bandwidth, broadband MMIC components, and miniaturized digital receivers. An effort is underway at AFRL to develop systems combining these elements, resulting in wideband phased arrays encompassing multiple receiver channels and capable of forming multiple beams through digital beamforming. The key elements of this effort revolve around three key areas: RF modeling, system integration, and system testing. The TELA Testbed allows for the integration of these technologies as a system that can be tested and verified through modeling. The ultimate goal is a broadband aperture simultaneously supporting EW, communications, and multiple radar modes. This approach will lead to reduced size, cost, weight, and power consumption while serving multiple simultaneous users with minimal impact on an airframe.

15. SUBJECT TERMS
Phased array, wideband array, wideband beamforming, digital beamforming, multi-channel receivers

16. SECURITY CLASSIFICATION OF:			17. LIMITATION OF ABSTRACT:	18. NUMBER OF PAGES	19a. NAME OF RESPONSIBLE PERSON (Monitor)
a. REPORT	b. ABSTRACT	c. THIS PAGE			Thomas W. Dalrymple
Unclassified	Unclassified	Unclassified	SAR	32	19b. TELEPHONE NUMBER *(Include Area Code)* N/A

TRANSFORMATIONAL ELEMENT LEVEL ARRAYS (TELA) TESTBED

Thomas Dalrymple, Jonathan Buck, Peter Buxa, John McCann, Robert Neidhard, Gary Scalzi, Caleb Shreffler, Dan Spendley, Paul Watson
Air Force Research Laboratory
2241 Avionics Circle, Bldg 620
Wright Patterson AFB, Ohio 45433

Abstract: The Air Force is in need of sensor technologies to support surveillance operations in complex Radio Frequency (RF) environments. Requirements dictate the need to find weak and strong scatterers simultaneously over broad bandwidth, while resolving emitter signal characteristics such as angle of arrival and time of arrival for signal identification and tracking.

Previous work at AFRL has resulted in many technologies that support these needs. Many components and subsystems exist today that were only theoretical a few years ago, such as phased array antennas that support 10:1 bandwidth, broadband MMIC components, and miniaturized digital receivers.

An effort is underway at AFRL to develop systems combining these elements, resulting in wideband phased arrays encompassing multiple receiver channels and capable of forming multiple beams through digital beamforming. The key elements of this effort revolve around three key areas: RF modeling, system integration, and system testing. The TELA Testbed allows for the integration of these technologies as a system that can be tested and verified through modeling.

The ultimate goal is a broadband aperture simultaneously supporting EW, communications, and multiple radar modes. This approach will lead to reduced size, cost, weight, and power consumption while serving multiple simultaneous users with minimal impact on an airframe.

1. Introduction

As the Air Force looks ahead to future threats and hardware needs, there is a constant push for more functionality and bandwidth from the various sensors used for radar, electronic warfare (EW), and communications. In the past, a state of the art radar or EW receiver would consist of a passive aperture with a fairly large analog backend receiver. These systems typically had a relatively small bandwidth. While many such systems are still in use today, phased array technology has been growing in use over the last 10 to 15 years. Active phased arrays containing low noise amplifiers and phase shifters have greatly increased the system performance available to the warfighter. These arrays

feature lower noise figures, multiple beams, and graceful degradation of performance as various elements fail over time. The receiver/exciter systems have evolved as well, increasing in bandwidth, incorporating multiple channels, and including some digital signal processing.

Now is the time to consider the future generation of these systems. Over the last decade many basic technologies have improved dramatically. Phased array antennas, formerly limited to 2:1 bandwidth, are now capable of greater than 10:1 bandwidth. Several groups, including Harris Corp., Raytheon, and Georgia Tech Research Institute, have produced and demonstrated arrays with these capabilities[1-2]. Broadband monolithic microwave integrated circuits (MMICs) also have greatly increased in capability. Some groups have reported up to 1 nanosecond of on-chip time delay for a true time delay MMIC design[3]. This MMIC is capable of covering a 10:1 frequency range, allowing element level broadband beamsteering up to ±60° for a one square foot phased array at X-Band. This type of technology also has great potential for reducing the complexity and the cost of integrating the hardware of the analog front end of a sensor.

Receiver technology has also continued to evolve over the last few years. Broadband block downconverters and tuners can cover from DC to 20 GHz with an output bandwidth of 500 MHz or higher. Also, engineers at AFRL have recently focused on developing "Receiver on a Chip" technology using silicon germanium and fully depleted silicon on insulator processes[4]. Plans in the near future will see the combination of broadband tuning capability combined with analog to digital converters (ADCs) on a single die. Even commercially available ADCs continue to push to higher levels of performance. Currently, off the shelf ADCs are capable of sampling 10 bits at greater than a two gigahertz sample rate.

Combining all of these elements – broadband phased arrays, broadband MMICs, and broadband digitizing receivers – is the emphasis of the Transformational Element Level Arrays (TELA) Testbed. Miniaturized receivers allow for multiple digital channels behind these broadband arrays. Applying digital beamforming to these digital channels can allow the system to create simultaneous beams to detect multiple signals without sacrificing performance. AFRL has been working on digital beamforming for many years, and has recently demonstrated a real-time beamforming system at X-Band[5]. These techniques will be applied to system demonstrations in the testbed.

As a home for broadband sensor technologies, the TELA Testbed will allow for a place to bring together all the components mentioned above for testing. The areas of focus – System Integration, RF System Modeling, and RF System Testing – will be described below. The initial work will focus on a 4-channel system also described below.

2. RF String Description

The initial demonstration of the TELA testbed is composed of several of the elements described above, including a wideband phased array antenna, low noise amplifier, a wideband block downconverter, and a multichannel high speed digitizer. A block diagram of a single RF channel (referred to as an RF String) is shown in Figure 1. The full receiver includes 4 channels digitized simultaneously. The band of interest for initial experiments is from 2 to 10 GHz.

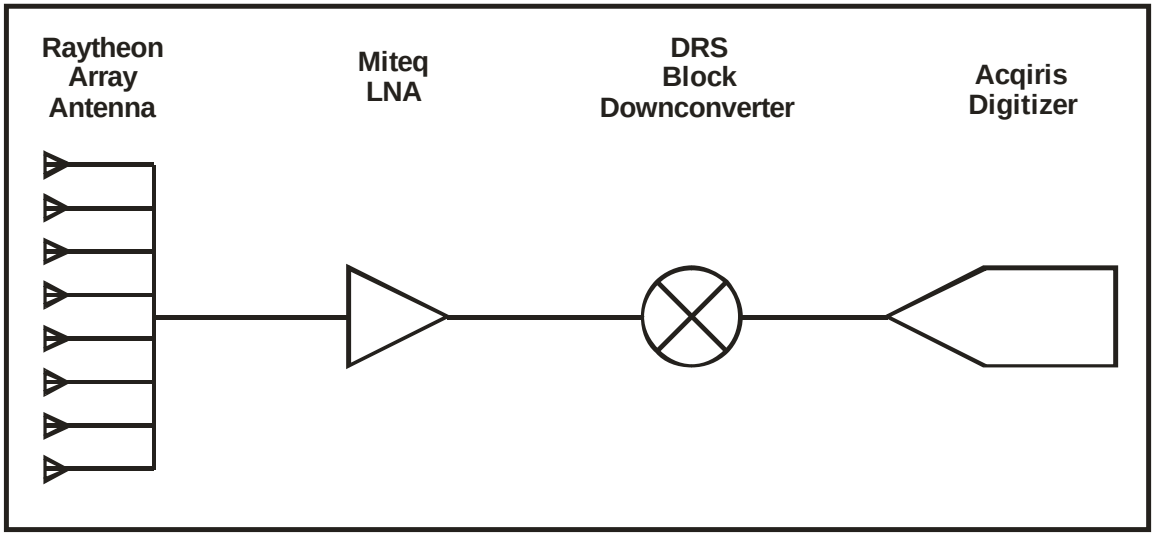

Figure 1: RF String Block Diagram

The Raytheon phased array was developed and delivered to AFRL under the DARPA RECAP program and covers 1.8 to 18 GHz. It is a 64-element array and has been configured in columns using passive power combiners. The array grid spacing is set to 0.325" in order to avoid grating lobes at the high end of the frequency range. This does not make for very attractive antenna patterns in the 2 to 10 GHz range, so the columns were set up to alternate between channel feeds and terminations, creating an effective element spacing of 0.650".

Each antenna column is fed through a Miteq LNA to set the noise floor for the system. The LNA provides 33 dB of gain and a 2 dB noise figure covering 2 to 10 GHz. The LNA is followed by a DRS SI-9250 block downconverter. The 9250 comes in a compact PCI format and covers 500 MHz to 18 GHz. The input RF is converted to a 1.6 GHz intermediate frequency (IF) with an 880 MHz bandwidth.

The final stage of the RF String is the four channel high speed digitizer, an Acqiris DC282. This digitizer comes in a compact PCI format, making it easy to integrate with the block downconverters for compactness and control of the system. Using an external

clock for our testing, the digitizer provides 10 bits of data at 2.133 GigaSamples/second. Data is captured simultaneously for the four channels and processed offline.

3. System Integration

System integration for the TELA testbed consists of integrating the Raytheon antenna, Miteq LNAs, DRS downconverters, and Acqiris digitizer in a 4-channel configuration. Control and testing of the whole receiver chain was accomplished by means of an onboard computer which was able to address the 4 block downconverters, 4-channel digitizer, and an external clock signal generator.

Figure 2 below shows how the individual components are integrated to form the RF strings. The Raytheon array is configured so that columns 2, 4, 6 and 8 are fed to the amplifiers. This doubles the element spacing and allows for improved antenna patterns in the 2-10 GHz range. The output of these four columns is then passed to the Miteq LNAs, which amplify the signal by ~33 dB. The amplified signal then passes through the SI-9250's and is downconverted to an Intermediate Frequency of 1.6 GHz with a ±440 MHz bandwidth. The IF signal is then digitized by the Acqiris DC282 at 2.133 GS/s with 10 bits of resolution in the 2nd Nyquist zone of the onboard Atmel ADCs. This digitized data is stored to a hard disk on the single board computer and displayed with the data acquisition software. The external 2.133 GHz clock is provided by an Anritsu signal generator.

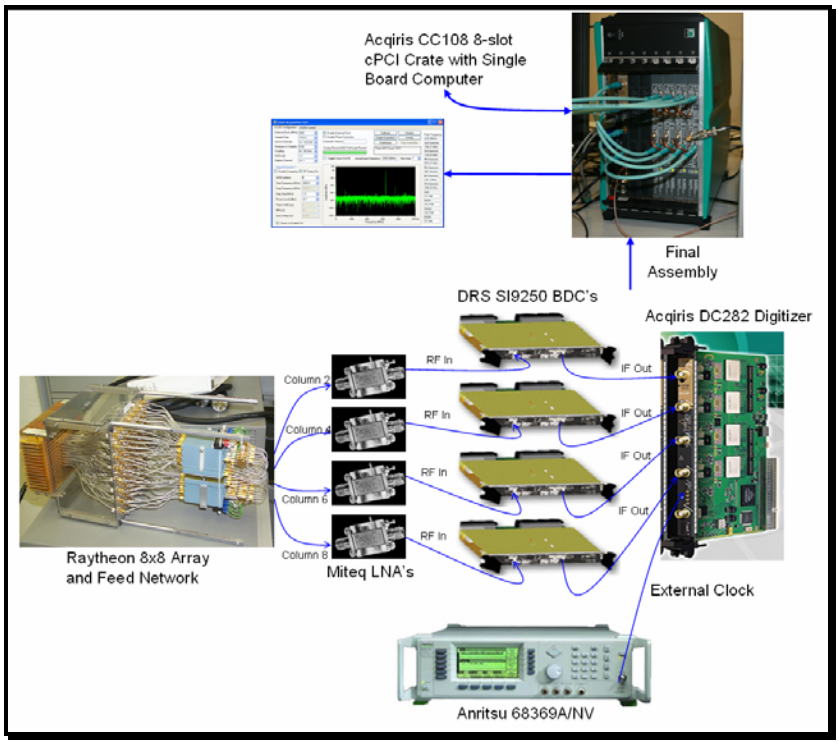

Figure 2: RF String Block Diagram

The devices that are software controlled include 4 DRS SI-9250 Block Downconverters, the Acqiris DC282 digitizer, and the external signal generator. These devices utilize the Compact PCI form factor and are installed in an 8-slot cPCI crate which also includes a Concurrent Technologies onboard computer.

The Acqiris DC282 is a 4-channel 10-bit digitizer with up to a 2.2 GS/s sample rate per channel when using an external clock source (2 GS/s max for internal clock). The full scale input voltages are user selectable and include 50 mV, 100 mV, 200 mV, 500 mV, 1 V, 2 V, and 5 V. Each channel can acquire up to 256 megasamples of continuous data, which translates to 120 ms of data using an external 2.133 GHz clock. The 4 channels can also be combined to achieve a sample rate of more than 8 GS/s. For all RF String testing the full scale voltage was kept constant at 500 mV which is the default setting for the onboard Atmel ADCs.

3.1 Software Integration

To interface with the SI-9250s, a driver was created using Jungo WinDriver™. This tool generated library functions that could be called from a C++ application. These library functions and the Application Programming Interface (API) provided by Acqiris were used to create the control software. The GUI was created with Visual C++ 2005 and utilizes tools from National Instruments Measurement Studio.

Figure 3 shows a screenshot of the main GUI window which is used to control the digitizer. The application programming interface (API) provided by Acqiris allows the user to control every aspect of the digitizer. The GUI allows the user to control the sample rate and external clock, active channels, channel combinations, number of samples, coupling, and full scale input voltage. The software has 3 data acquisition modes; Single, Continuous, and Sweep. Single mode simply acquires the requested number of samples, computes the FFT and writes the digitized data to a file. Continuous mode repeatedly collects the requested number of samples and computes the FFT and does not write the data to a file. Sweep mode utilizes a GPIB-attached signal generator and sweeps across a user defined range of frequencies. As the signal is swept, data is collected, the FFT is computed, and the data is stored to a file. For all 3 modes, the signal harmonics as well as Spur Free Dynamic Range, Signal to Noise Ratio, Signal to Noise And Distortion, and Effective Number of Bits of the digitizer are computed and displayed. The full scale percentage is also monitored so that the user can see if they are overpowering the digitizer. The frequency spectrum is generated using the National Instruments Measurement Studio Signal Processing library and a scatter plot.

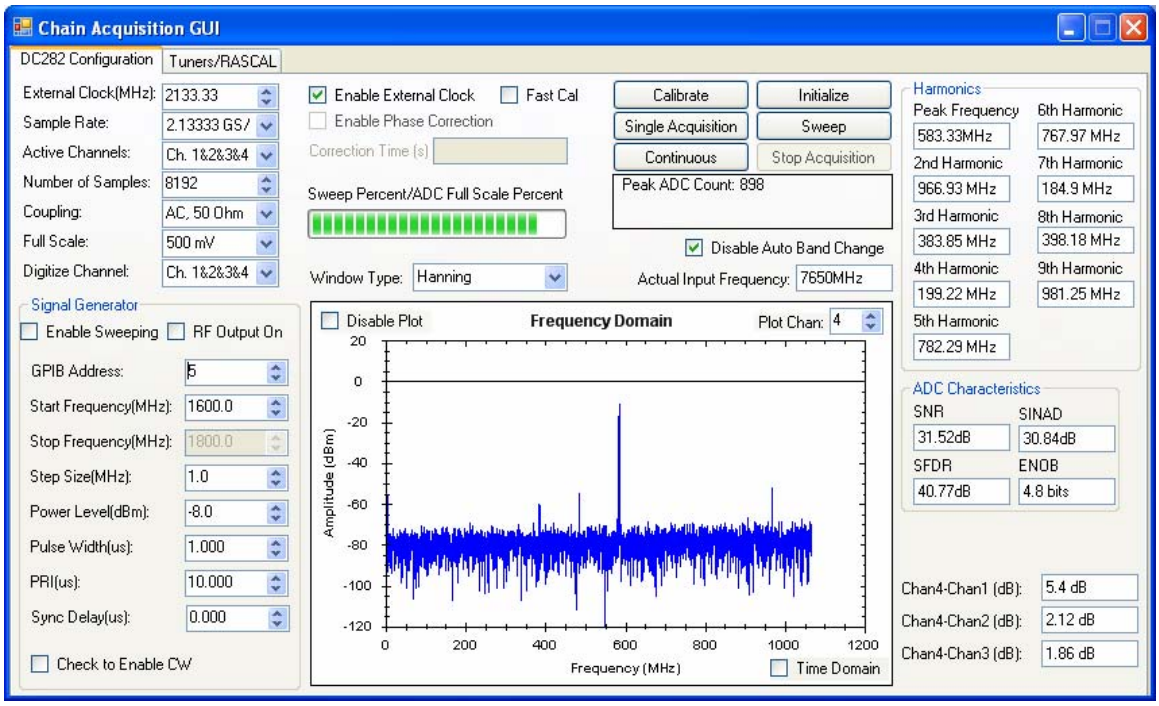

Figure 3: Acqiris Control GUI

Figure 4 shows the GUI which is used to control the DRS Block Downconverters. When executed, the software searches the PCI bus using generated library functions for any devices that are installed in slots 5-8 of the Acqiris MAQbox cPCI chassis. If there is a device installed in a slot, the checkbox for that slot is enabled so that the user can select it and send commands. To change the band of the selected tuner(s), the user simply selects one of the bands from the drop down list and the appropriate commands are sent to the device.

The software also has the ability to automatically change the band of the downconverters. This is done by comparing the calculated actual input frequency to the edges of a band. If a signal crosses the edge of a frequency band, the program will automatically switch the tuner band to the next one higher or lower depending on which edge the signal crossed.

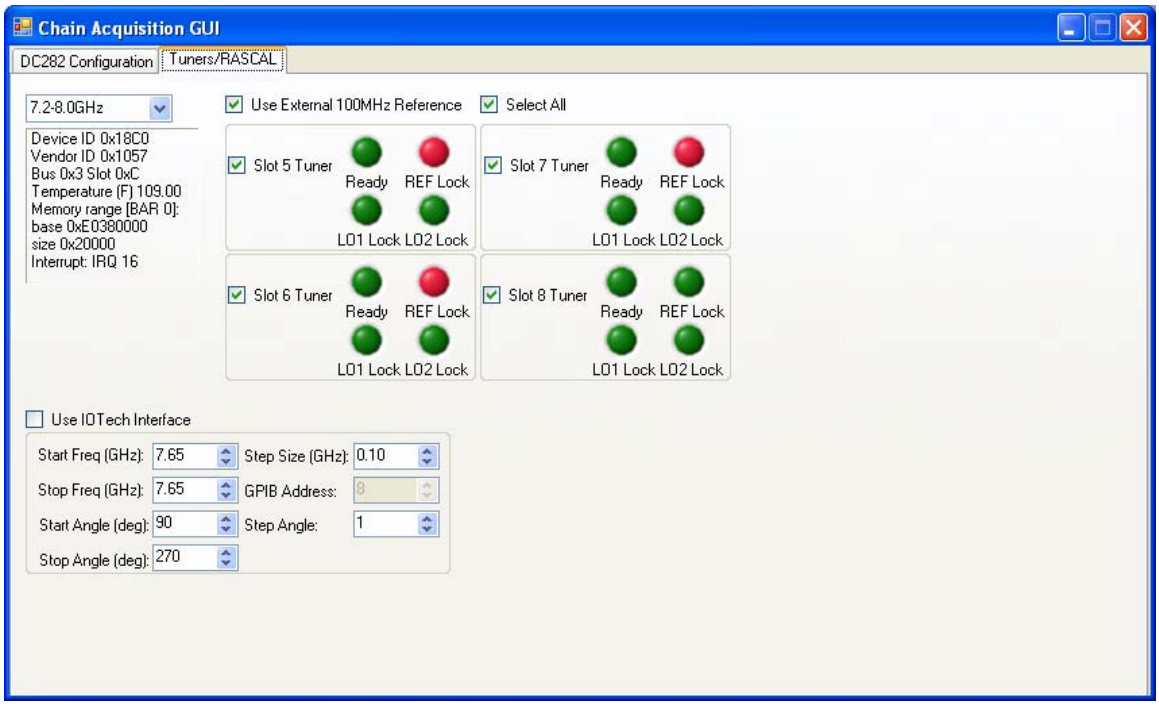

Figure 4: SI-9250 Control GUI

4. RF System Modeling

A combination of linear and nonlinear RF modeling is essential for gaining an understanding of system performance issues and identifying possible improvements before implementation in hardware. Modeling can be performed in a hierarchal fashion depending on the desired accuracy of the simulation. A typical approach is to begin with cascaded 2-port analysis, then move towards behavioral modeling of components, and finally with circuit level modeling. Cascaded 2-port analysis is the least computationally expensive, but also the least accurate. Circuit level modeling is the most accurate, but the most computationally expensive. Behavioral modeling is a compromise between the two. All levels of modeling are useful, depending on where one is in the design cycle.

Cascaded 2-port and behavioral modeling and analysis of a single RF string, consisting of an antenna element (1x8 column), a Miteq LNA, and a DRS block downconverter, has been performed in order to provide the correct input signal levels to the Acqiris digitizer, as well as to assess performance parameters such as spurious-free dynamic range (SFDR), minimum detectable signal (MDS), noise figure (NF), gain, and receiver saturation characteristics. The SFDR is bounded in minimum signal detection by noise and maximum signal detection by unacceptable in-band distortion. In our case, this corresponds to the difference between the MDS and the input signal which produces third-order intermodulation (IM3) products which are equal the noise level at the output of the chain. Third-order intermodulation products are of primary importance because

they appear within the bandwidth of the desired signal and cannot be filtered out. For a more detailed discussion of receiver chain analysis see [Pozar][6]. Once a sufficient level of modeling accuracy has been achieved, different operating scenarios can be simulated and performance can be assessed.

4.1 Cascaded 2-Port Analysis

Initially, cascaded 2-port analysis of the Miteq LNA and the DRS downconverter was performed using a commercially available tool, Syscalc[7], shown in Figure 5. In this manner, initial performance estimates were established. Datasheet parameters at an RF frequency of 5.2 GHz for the Miteq LNA (NF= 2 dB, gain= 33 dB, OIP3= 27 dBm) and the DRS downconverter (NF= 17.5 dB, gain= 9 dB, and OIP3= 16 dBm) were input into the program. The bandwidth was set at 880 MHz with an IF frequency of 1.6 GHz. Cascaded NF, gain, and OIP3 were 2.08 dB, 42 dB, and 15.96 dBm, respectively. The analysis shows a SFDR of 37.61 dB with a MDS of -82.46 dBm. In order to avoid distortion, the maximum input signal level is near -45 dBm. The output power for the -45 dBm input is -3 dBm which maps well to the maximum input signal of the digitizer of -2 dBm (500mV peak to peak, 50Ω). The SFDR is limited by two factors, the noise floor due to the large bandwidth and the low OIP3 of the downconverter.

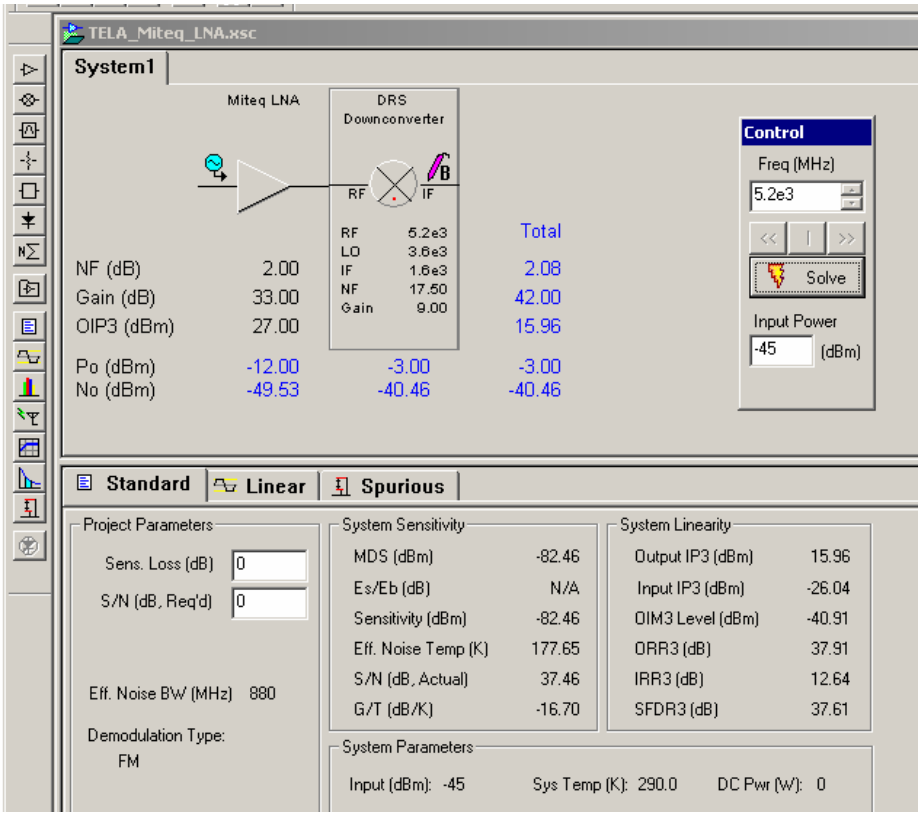

Figure 5: Cascaded 2-port analysis of LNA plus downconverter box

If instead of integrating the noise power over the full 880 MHz bandwidth one were to reduce the resolution bandwidth in the digitizer by using an FFT approach, the noise floor would be decreased, thereby improving, the SFDR significantly. The result is shown in Figure 6 with a resolution bandwidth of 0.2604 MHz, corresponding to a sampling frequency of 2.133 GHz using a 8192 sample FFT. The SFDR is now 61.13 dB with a MDS of -117.75 dBm. The maximum input signal for distortion free performance is now -56.62 dBm.

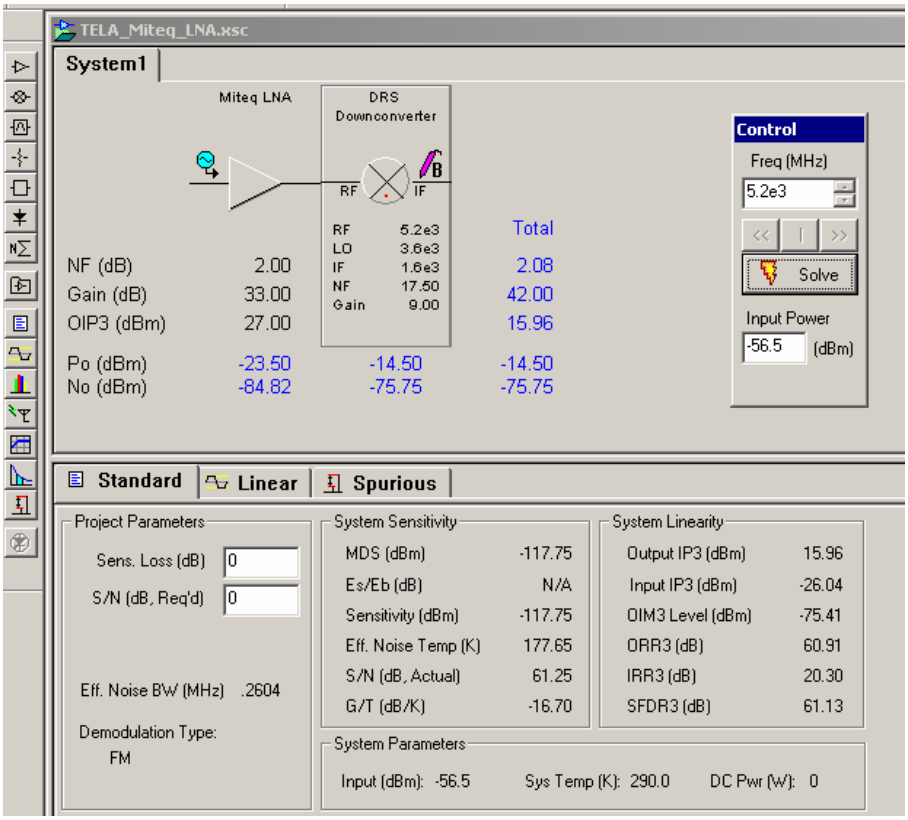

Figure 6: Cascaded 2-port analysis of LNA plus downconverter box with resolution bandwidth reduced from 880 MHz to 0.2604 MHz in the digitizer

4.2 Behavioral Modeling

While cascaded 2-port analysis provides valuable insights into expected system performance, it is limited in accuracy. A significant limitation for this work (2- 10 GHz) is the lack of frequency dependent analysis capability. Moving towards more accurate modeling over frequency, behavioral models were developed and analyzed in Agilent's ADS[8] CAD software.

Behavioral modeling of the Miteq LNA was accomplished using measured S-parameter data, NF data, power compression data, and 2-tone intermodulation data over the

frequency range of interest. Models were implemented with a table-based approach, utilizing interpolation between measured data points. Nonlinearities were modeled using 9th order polynomials. As an example of added model fidelity, Figure 7 shows simulated power compression curves at 2 GHz, 5GHz, and 8 GHz. Note that gain, compression characteristics, and nonlinear effects show some frequency dependency.

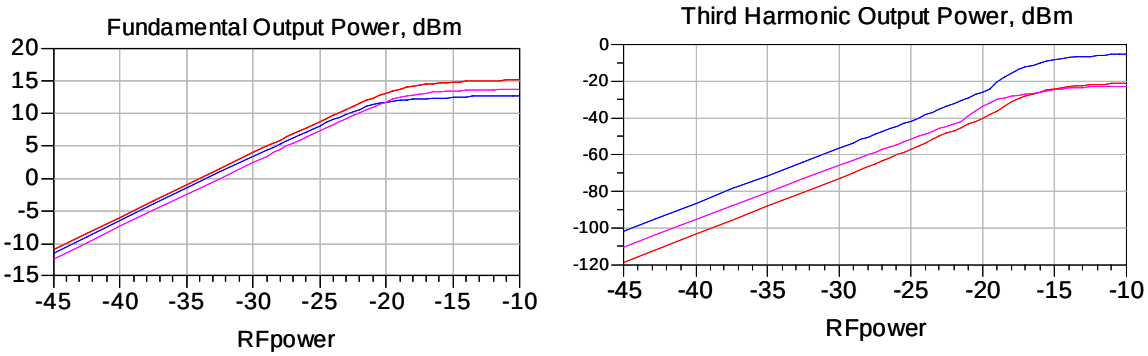

Figure 7: Fundamental and third harmonic power curves at 2 GHz, 5 GHz, and 8 GHz

The DRS downconverter has been modeled as an ideal mixer followed by a non-ideal amplifier, including second and third-order effects. Filters are also included to limit the bandwidth to that of the actual downconverter. In this manner, the fundamental and third-order intermodulation responses, which fall within the IF (output) bandwidth, can be accurately predicted. Modeling in this fashion is a reasonable approach due to the conversion process and filtering available in the downconverter. Detailed data regarding the individual components inside the unit were not available. Gain, NF, IP2, and IP3 measurements were taken in the various frequency bands of the downconverter and stored as a table-based model. The value of the parameters used is dependent on the specific downconverter unit and the frequency band chosen for analysis.

The behavioral models for the Miteq amplifier and the DRS downconverter have been combined and simulated using Harmonic Balance and Circuit Envelope methods available within Agilent ADS, as shown in Figure 8. As an example of the modeling capability, a 2-tone intermodulation analysis centered at a 5.1 GHz input frequency was run. Figure 9 shows the output of the simulation, where the X-axis represents the offset in MHz from the 1.6 GHz IF frequency. The input power for each carrier was -56 dBm and the tone spacing was set at 10 MHz. Markers 1 and 2 are the fundamental tones, while markers 3 and 4 are the third-order intermodulation tones. Resolution bandwidth for the noise floor is approximately 300 KHz. Simulated and measured results compare very well as demonstrated in Table 1. Also, results from a Syscalc analysis utilizing measured component parameters are also given for comparison.

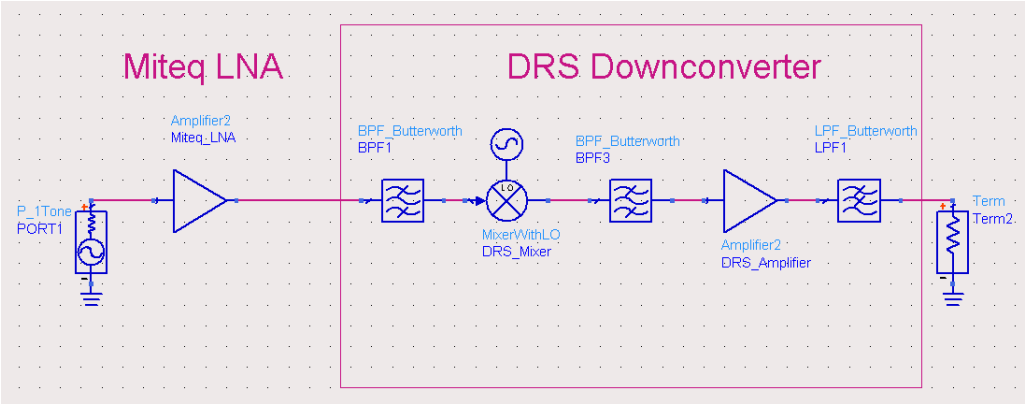

Figure 8: Simulation setup for behavioral modeling of LNA plus downconverter

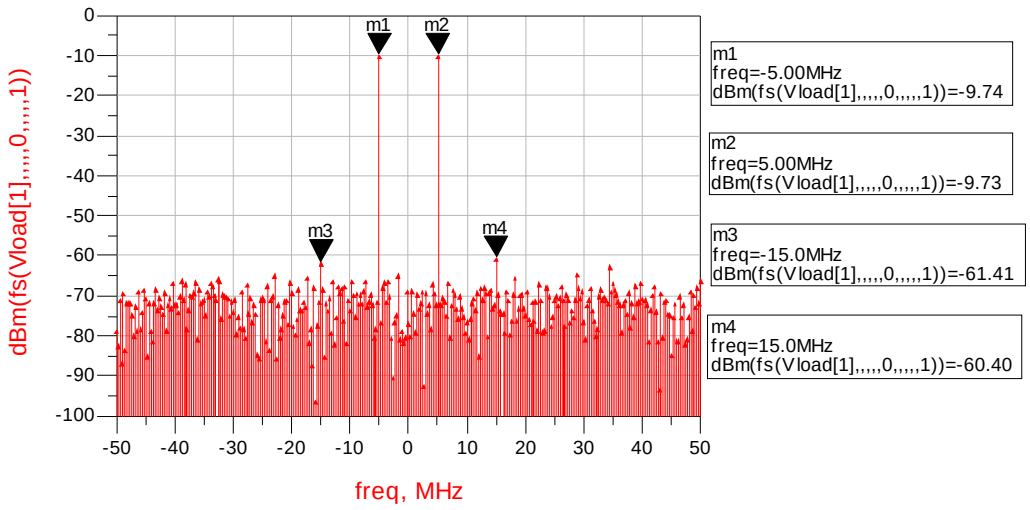

Figure 9: Simulated 2-tone response of Miteq LNA plus DRS downconverter. Input power is -56 dBm with a tone spacing of 10 MHz. Resolution bandwidth =300 KHz

Table 1: Simulated and measured performance for the Miteq LNA plus DRS downconverter. Shown are gain, output noise power (No), output third-order intercept point (OIP3), signal-to-noise ratio (SNR), spurious-free dynamic range (SFDR), and minimum detectable signal (MDS). Resolution BW = 300 KHz

	Gain (dB)	No (dBm)	OIP3 (dBm)	SNR (dB)	SFDR (dB)	MDS (dBm)
Behavioral	46.4	-71.1	16.1	61.4	58.1	-117.5
Measured	46.7	-72 (Avg. 100)	16.2	62.7	58.8	-118.7
Cascaded 2-port	46.3	-70.5	16.3	60.84	57.9	-116.8

Even though there is not a large difference between the cascaded 2-port and behavioral modeling approaches, it must be noted that the input signals here are relatively simple 1-tone or 2-tone. Behavioral modeling will be much more valuable with complex signals which occupy a greater portion of the frequency spectrum (ex. LFM) or when examining effects of intentional or unintentional interfering signals.

Angle of arrival dependent effects can also be modeled for the antenna described in Section 2. Pattern measurements have been taken, as described in Section 5, and form the basis of a table-based behavioral model which can be incorporated into the RF string simulation as shown in Figure 10. Figure 11 shows a simulation of column 2 of the antenna over a frequency range of 5.1 GHz to 10.1 GHz in 1 GHz steps where 90° corresponds to broadside. Interpolation is utilized between measured points. Using this data, the dynamic range of the RF chain can be mapped to the range of electric field intensity present at the face of the antenna for desired operation characteristics.

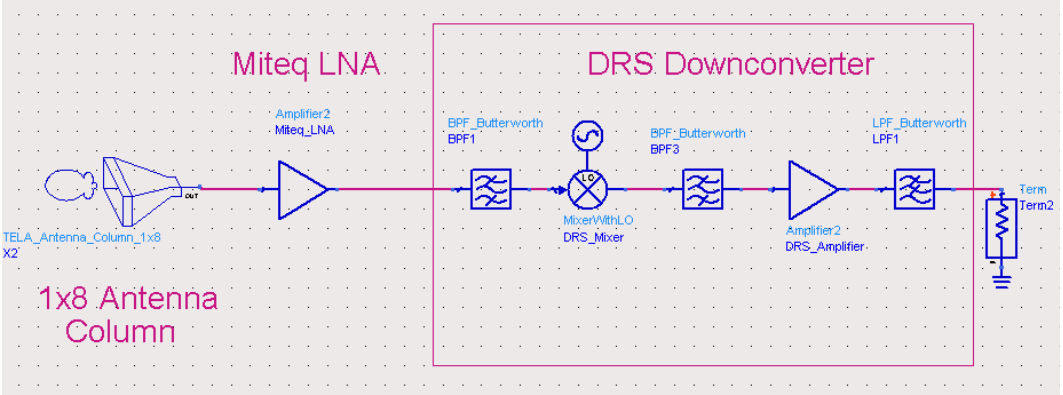

Figure 10: Simulation setup for behavioral modeling of 1x8 antenna column, Miteq LNA, and DRS downconverter

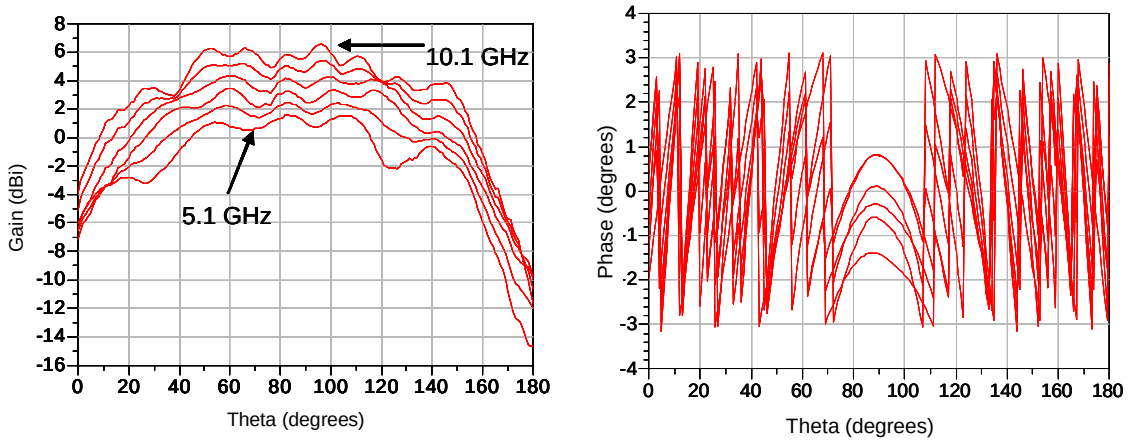

Figure 11: Simulated radiation pattern for column 2 of array over 5.1 GHz to 10.1 GHz

It must be noted that the current simulations do not include undesired effects introduced by the digitizer such as added noise and distortion when performing the analog-to-digital conversion. Effects such as these need to be taken into account and will degrade the performance of the receiver. Future work is planned in this subject area.

5. RF System Testing

5.1 Analog Testing & Beamforming

In order to test the integration of these multiple technologies, the ability to accurately characterize an antenna array is a necessity. Antenna measurements typically require that the source antenna and the antenna (or object) under test be separated by a large distance. This ensures that the target is illuminated by a locally planar wavefront, a condition that complies with definitions of antenna patterns and radar cross section. Furthermore, since antennas are designed to convey energy over large distances, the locally planar wavefront simulates real operating conditions. On the other hand, an indoor facility allows testing to take place in a secure environment, regardless of weather conditions. To generate a uniform plane wave in a limited amount of space, a compact range employs a feed-reflector system within an absorber-lined anechoic chamber. A diagram of a typical compact chamber is shown in Figure 12. AFRL's Radiation and Scattering Compact Antenna Laboratory (RASCAL) is equipped with a precision rolled-edge reflector that collimates the impinging spherical wave from an offset feed resulting into a uniform plane wave. The reflector is housed in an aluminum enclosure (24 feet long, 12 feet wide, and 9 feet high). In addition, the walls are lined with a curved pyramidal and curved wedge absorber. RASCAL currently has the capability to measure antenna gains and radiation patterns in the 2-18 GHz frequency band with high fidelity. RASCAL utilizes an Agilent 8362B Network Analyzer for fully automated data acquisition. RASCAL also uses an Agilent 8510 Vector Network Analyzer for S-Parameter measurements.

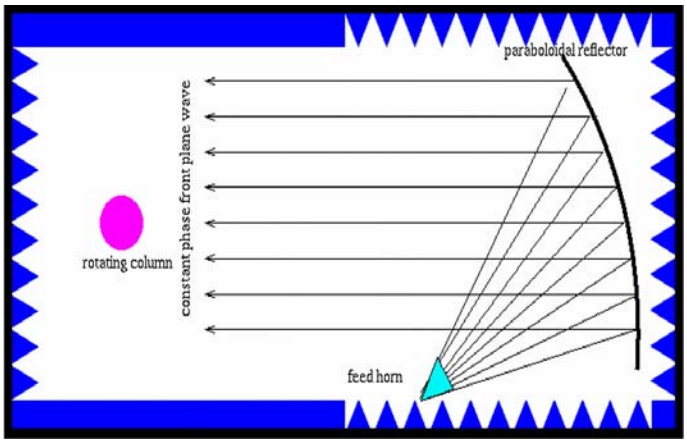

Figure 12: Depiction of a typical compact antenna range

As mentioned in Section 2, the antenna used in this effort is a wideband array procured from Raytheon. The Raytheon array employs a flared notch element. For full polarization selectability, a second set of boards is interleaved at ninety degree angles to the first. The result is the egg crate structure shown in Figure 13. Raytheon built and delivered an array with 16 x 21 dual polarized elements, yet only the 8 x 8 sub-array in the center was connectorized. With two separately fed polarizations, there are 128 connectors overall. The remaining elements were resistively terminated.

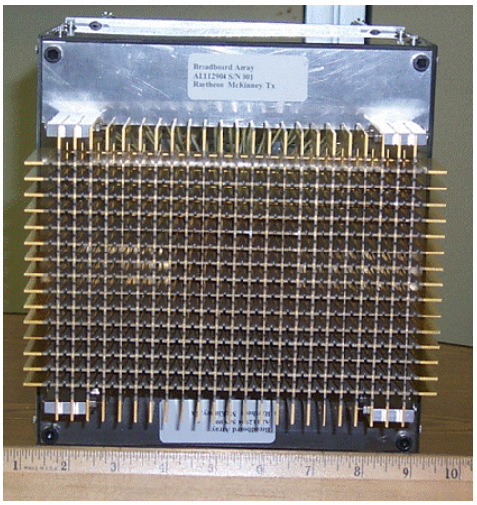

Figure 13: The egg crate structure of the front face of the Raytheon array.

The RF system testing in this effort required the configuration of the Raytheon array into four channels. The configuration chosen was four 8-element columns. As stated in Section 2, since these tests were performed at the low end of the array's operating frequency range, the array's eight columns alternated between feeds and terminations. A block diagram of the feed structure used in this effort is shown in Figure 14. It is broken down into three sections: the 32-element (four eight-element columns) array, the 8:1 combining network that defines the four channels, and the analog beamforming network. The analog beamforming network was used to take sum and difference antenna patterns of the entire array to compare to the results of the digital beamforming. Figure 15 shows a close-up view of the feed structure behind the array and the test setup in RASCAL.

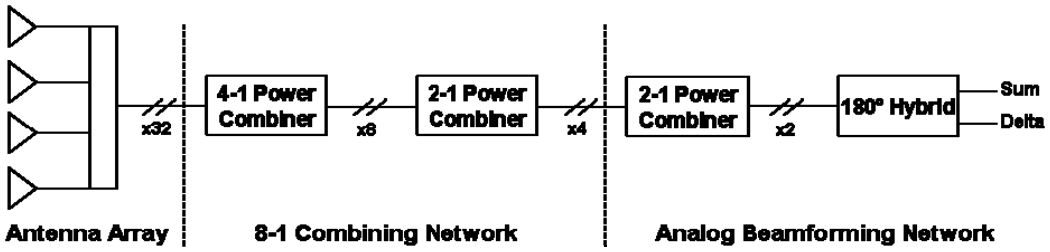

Figure 14: Block diagram of feed structure behind Raytheon array

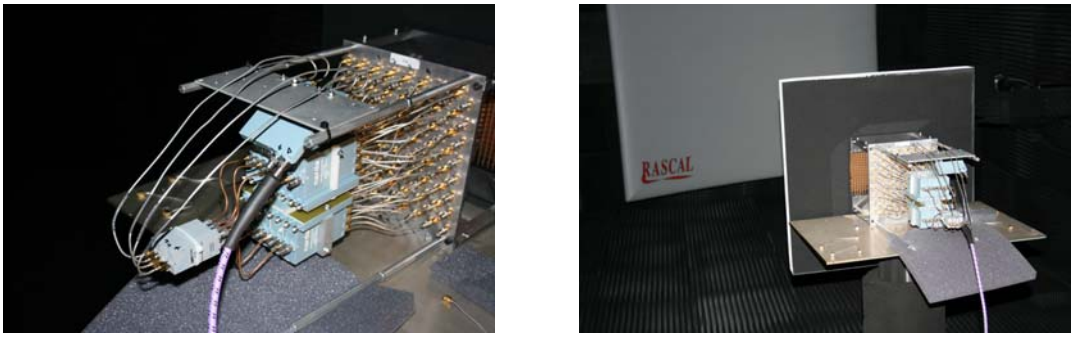

(a) (b)

Figure 15: Close-up view of the feed structure behind the array (a) and the test setup in RASCAL (b)

In order to characterize the feed structure of the antenna, swept S-parameter measurements from 2-12 GHz were taken using RASCAL's Agilent 8510 Vector Network Analyzer. Return loss versus frequency of the four individual channels is shown if Figure 16a, and return loss of each of the sum and delta ports of the 180° hybrid is shown in Figure 16b. It is evident from Figure 16 that the antenna performance (with regards to matching) drops off at the lower frequencies (around 2-5 GHz). Figure 17a shows the insertion loss through one channel of the 8:1 combining network. The results are as expected, with loss being slightly over 9 dB and increasing with frequency. Figure 17b shows the insertion loss through both the analog beamforming network and the 8:1 combining network. These results are also as expected, with about 6 dB more loss coming from the extra 4:1 power dividing.

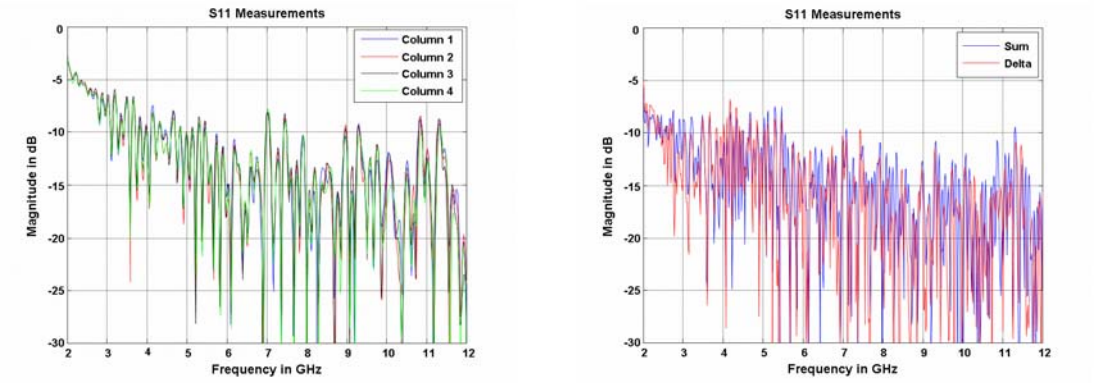

(a) (b)

Figure 16: Return loss at each of the ports of the antenna feed structure, the four channels of the 8:1 combining network (a), and the two ports of the analog beamforming network (b)

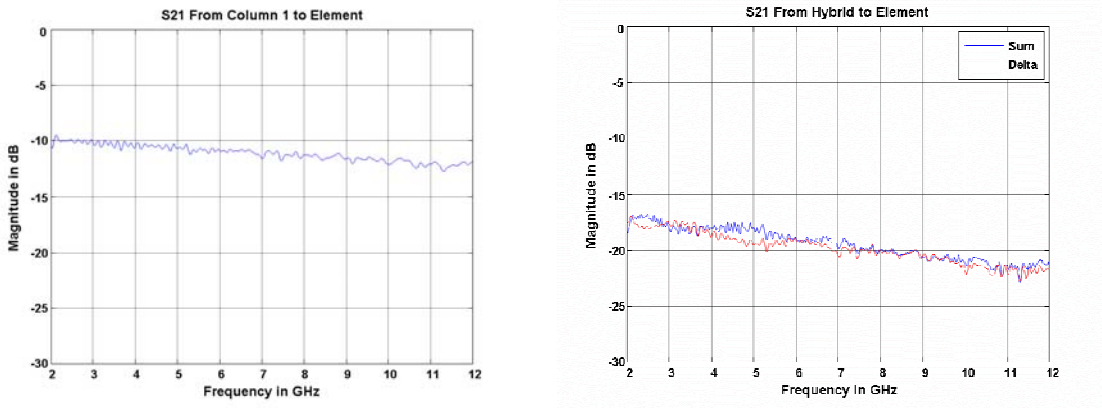

(a) (b)

Figure 17: Insertion loss through one channel of the 8:1 combining network (a) and through both the analog beamforming network and 8:1 combining network

Antenna pattern measurements were conducted in RASCAL from 2-12 GHz, with the Raytheon array setup to scan at broadside. The orientation in the compact range is such that boresight (the antenna looking directly at the reflector) is labeled 180°. Elevation cuts of 90° to 270° were taken. Standard gain horn measurements were also taken to calibrate the gain of the antenna to dBi. This gain also includes the insertion loss discussed above. Figures 18, 19, and 20 show antenna patterns at 5.10 GHz, 7.5 GHz, and 10.2 GHz, respectively. The patterns included are calibrated gain and phase of each individual channel as well as the calibrated sum and difference patterns (the output of the analog beamforming network).

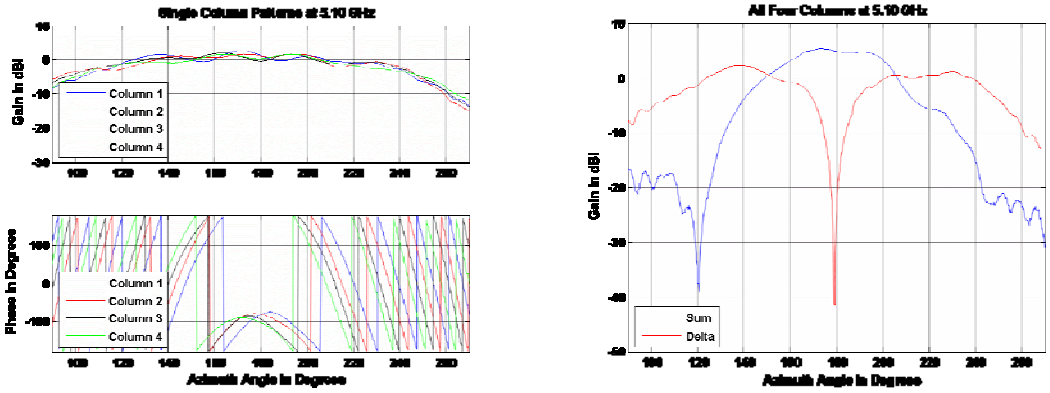

(a) (b)

Figure 18: Single-column gain and phase (a) and combined sum and difference patterns (b) at 5.1 GHz

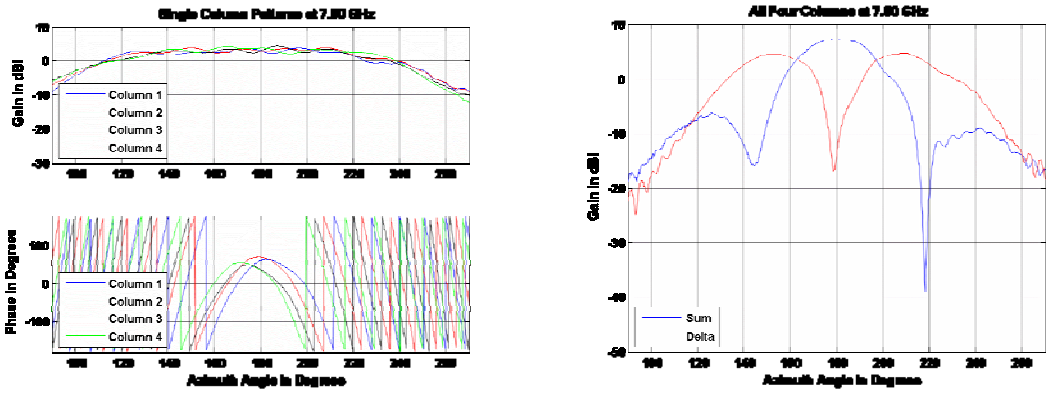

(a) (b)

Figure 19: Single-column gain and phase (a) and combined sum and difference patterns (b) at 7.5 GHz

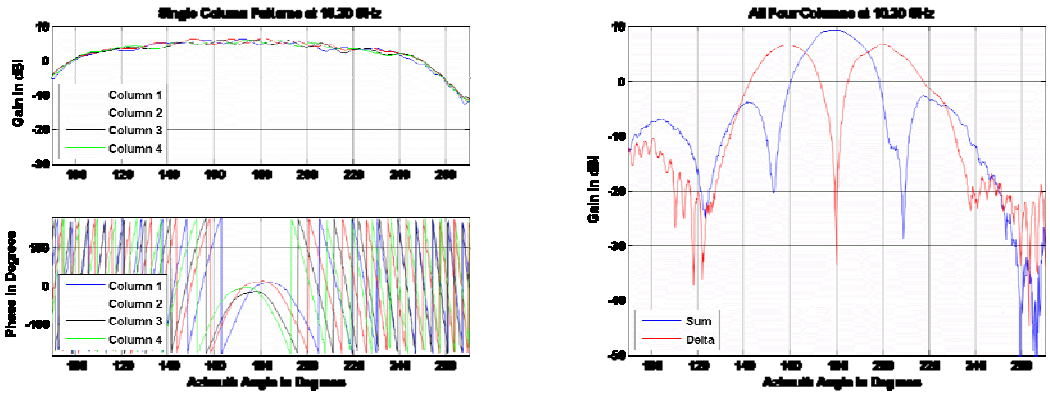

(a) (b)

Figure 20: Single-column gain and phase (a) and combined sum and difference patterns (b) at 10.2 GHz

5.2. Digital Testing and Beamforming

Following the analog characterization of the antenna array, the full 4-channel digital receiver chain was set up in the RASCAL chamber. This included all of the RF String hardware as described in earlier sections. For digital testing purposes, a GPIB to Digital TTL converter box, manufactured by IOTech, was used to communicate with the range software. During a scan, the range software would send digital triggers to the IOTech box. These triggers were read over GPIB by the RF String control software and used to determine when the antenna was set at a specific angle/frequency so that data could be acquired. The current scan angle and frequency were also read over GPIB and incorporated into the filename for each data acquisition. A diagram of the test setup is shown in Figure 21.

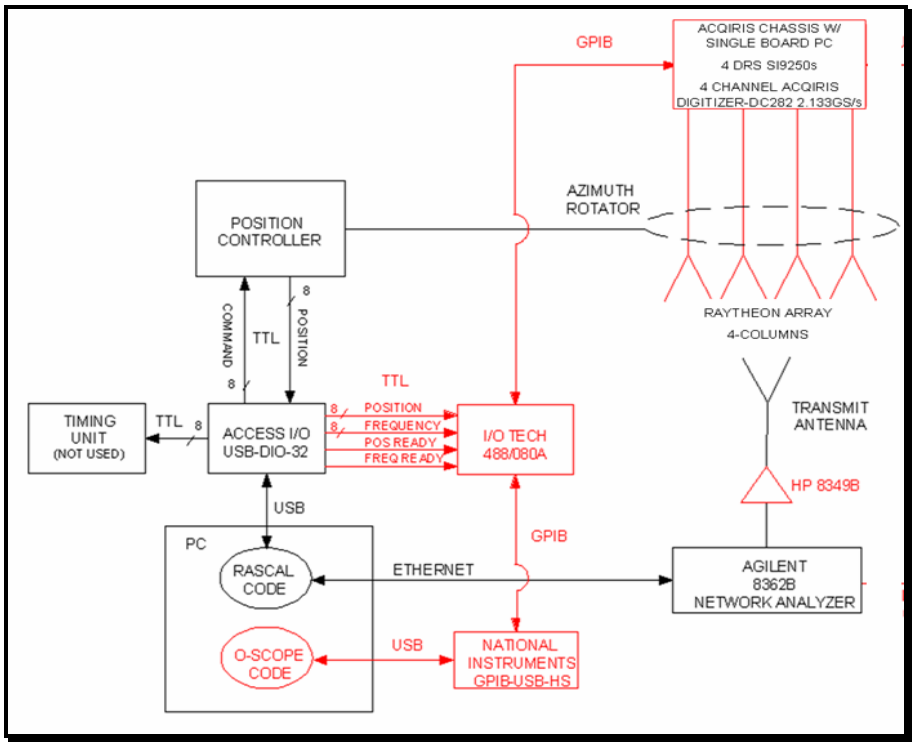

Figure 21: RASCAL Test Setup

5.2.1 Digital Calibration and Beamforming

As seen in the previous sections, the received signals from the phased-array are passed through wideband RF down-converters and then digitized at 2.133 GS/s with 10-bits of resolution. The digitized data is then recorded in a separate hard-drive to be processed off-line. This technique is often referred to as “poor-man’s DBF”, alluding to the fact that only a minimal amount of hardware is necessary since all processing is performed in software. This post-processing approach is appropriate for a laboratory environment, but in an operational environment it would be desirable to process the data in a near-real-time

fashion. This approach does lack the "real-time" feel of a digital beamforming system, but nonetheless provides a solid stepping stone in which to base initial system performance estimates and future directions for the testbed's digital hardware.

The initial RF-string tests have solely focused on continuous-wave signals, enabling the processing algorithms to utilize the narrow-band array model common to the beamforming literature[9]. The model provides a great advantage for the initial tests in that array calibration and beam steering can be performed using phase shifts rather than fractional-delay sampling filters, integer-sample delays, or other wideband processing techniques. Due to the digitizer's real output format, as opposed to a complex valued output stream, all calibration and weighting was performed in the frequency domain. This is a simple and well-known beamforming approach that, although requiring computationally intense Fast-Fourier-Transform (FFT) to extract the narrowband signal of interest, the resulting data can be simply weighted by a single complex multiplication. Once the data has been weighted, the user has the option to either continue processing in the frequency domain, or convert the data back into the time domain using the Inverse-Fast-Fourier-Transform (IFFT) for further processing. Figure 22 provides a basic block diagram of a beamforming system which processes the weighted data in the frequency domain.

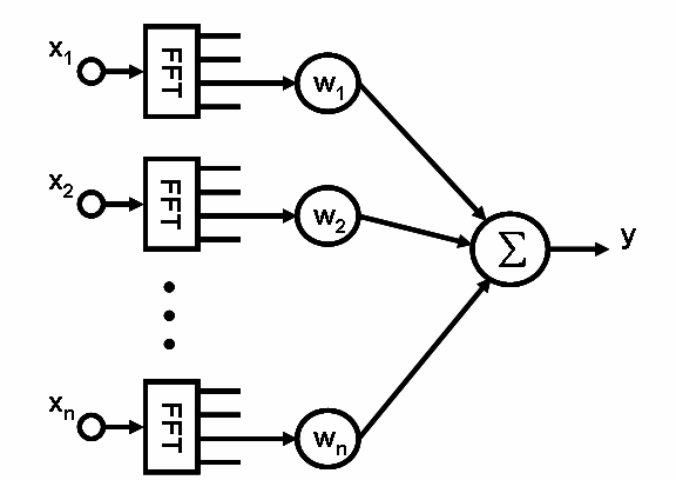

Figure 22: Narrowband Frequency Domain Beamformer

Although the analog components of the RF-String were demonstrated to have excellent magnitude and phase matching properties, the addition of the digital circuitry creates unacceptable phase and amplitude mismatches as seen in the top plot of Figure 23. Mismatches of these magnitudes are unable to produce the desired array patterns and thus need to be minimized using digital calibration. By applying the narrowband assumption, a similar calibration procedure as used in [5] was applied. Using the raw data collected at broadside, each channel's narrowband response is measured using the FFT. One channel is then selected as the reference to which all channels are normalized resulting in a

uniform phase front at broadside as shown in the bottom plot of Figure 23. The center plot of Figure 23 shows the phase matching of the four channels prior to amplitude correction. The amplitude correction can be performed as a separate step or be included in the phase correction adjustment. The resulting normalization weights are then applied to their respective channel's recorded data at all other measured angles to correct for the phase and magnitude mismatches.

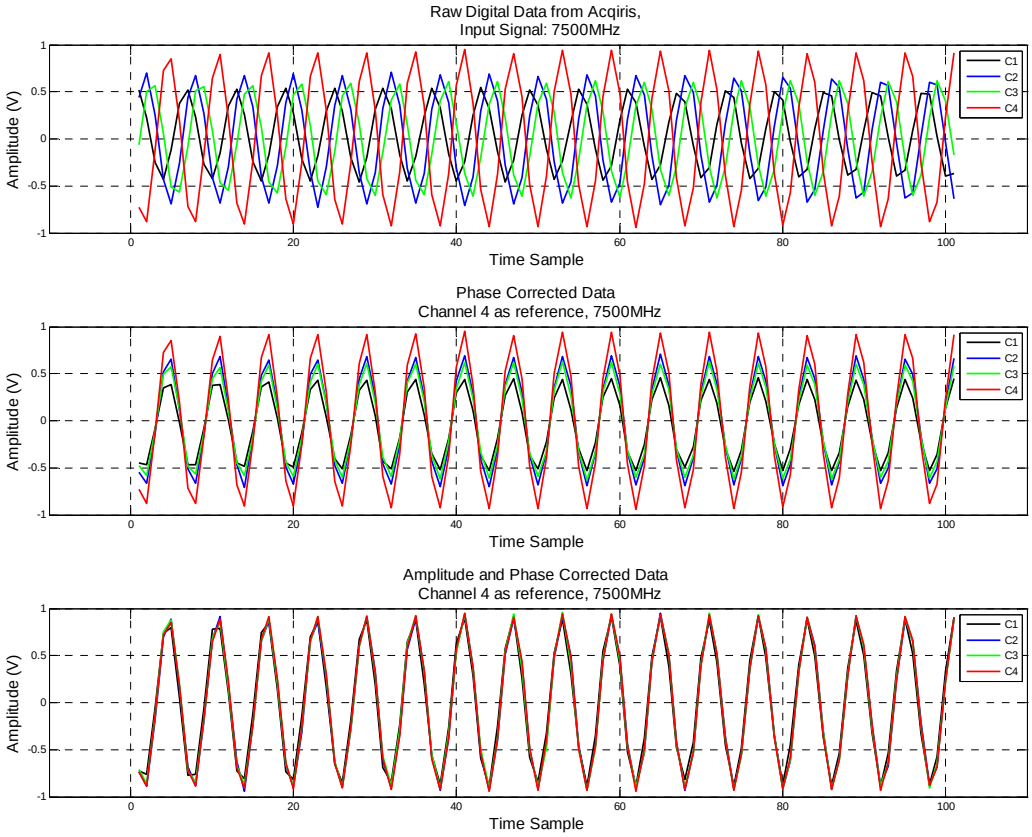

Figure 23: MATLAB Calibration Steps for Boresight Data at 7.5GHz

Due to the narrowband assumption, calibration was performed for each frequency in which the RF-string was tested. Once the calibration weights were calculated, it was possible to accurately apply linear-phase progressions across the array in order to perform beam steering. To ensure the calibration and beam steering was being performed accurately, the channel summation was processed in both the frequency and time domains. The resultant array patterns were then inspected and found to contain only slight differences, providing evidence that the implemented digital beamforming algorithms were working correctly.

5.2.2 Measured Results

Since the array was designed for 60-degree grating-lobe free scans at the upper-end of the system bandwidth, 18 GHz, and the array testing was performed in the lower-range of the system bandwidth, array patterns measured using consecutive columns lacked any clear array pattern definition. To present a more aesthetically pleasing final result, the spacing between columns was increased from using every consecutive output, to using every other column output. This technique doubled the spacing between the active columns and better approximated a half-wavelength spaced array for the frequencies under test. The measured array patterns for all frequencies were then compared to corresponding experimental simulations.

A subset of the measurements and simulations are shown below in Figures 24 and 25. For reference purposes, the measured and corresponding simulated array patterns are displayed on the same axes. The simulated patterns were modeled using a standard cosine element pattern along with the physical array architecture. The simulation versions did differ from the measured patterns, but provided a baseline as to the array pattern's basic shape and tendencies. It was noted that the measured and simulated patterns correlate well for all measured frequencies and steered look directions.

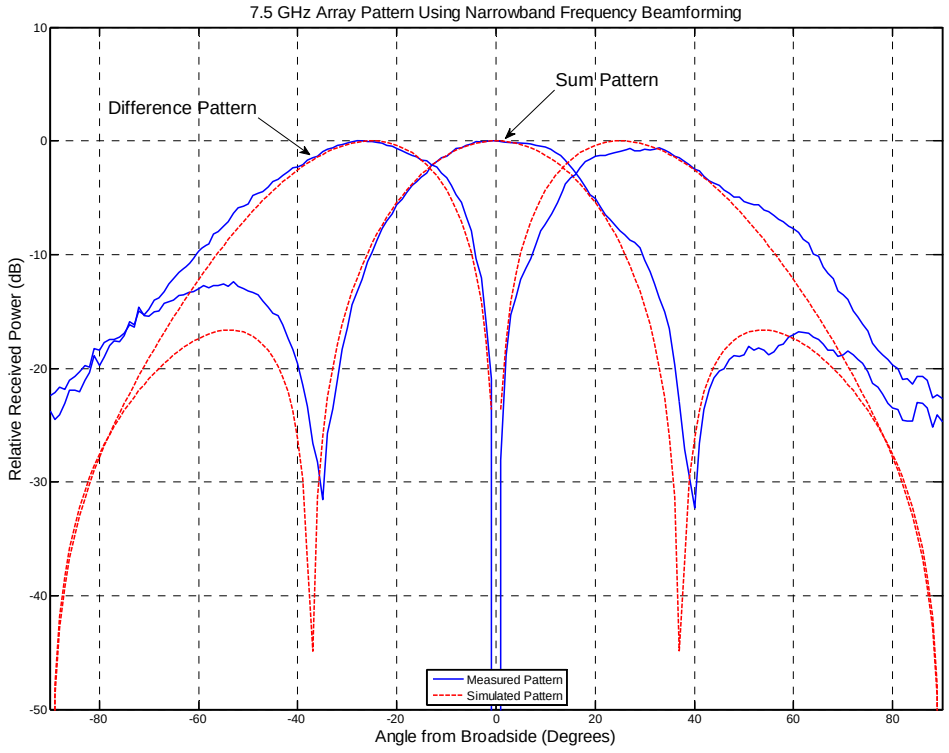

Figure 24: Broadside Array Pattern

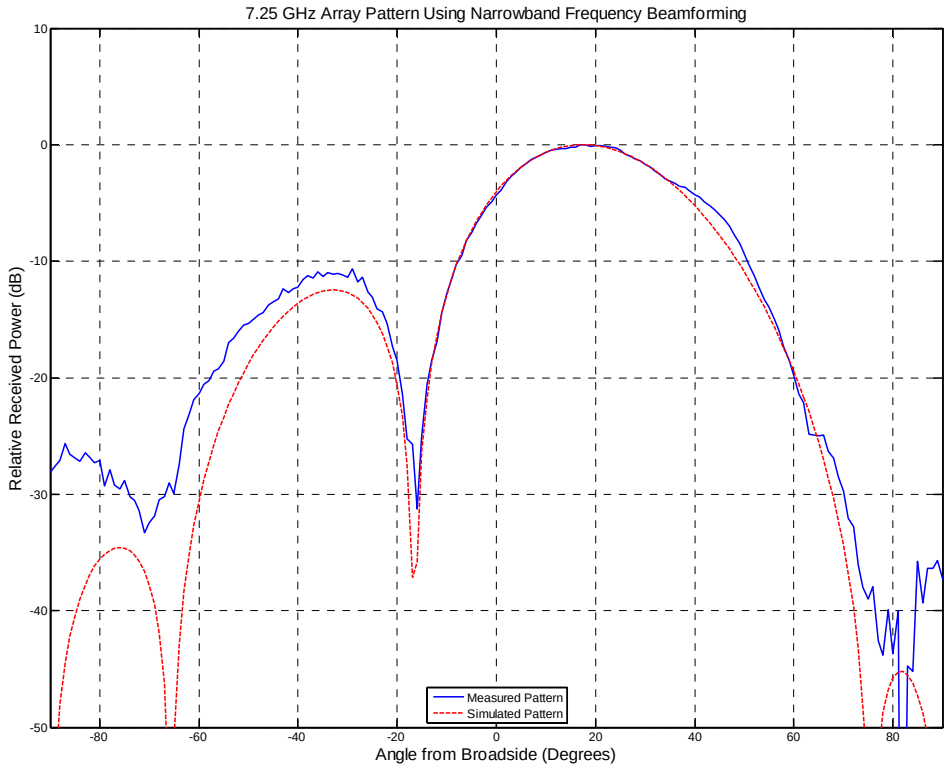

Figure 25: Scanned Array Pattern

For a direct comparison between analog and digital beamforming measurements, an attempt was made to replicate the sum and difference patterns shown in Figures 18-20 using digital beamforming. Figure 26-28 present the measured digital patterns overlaid onto the original analog measurements for a carrier frequencies of 5.2 GHz, 7.5 GHz, and 10.1 GHz. These measurements, along with similar patterns taken across the tested bandwidth, provide both proof and confidence that the wideband test bed is fully operational for our immediate testing purposes from 2 to 10 GHz.

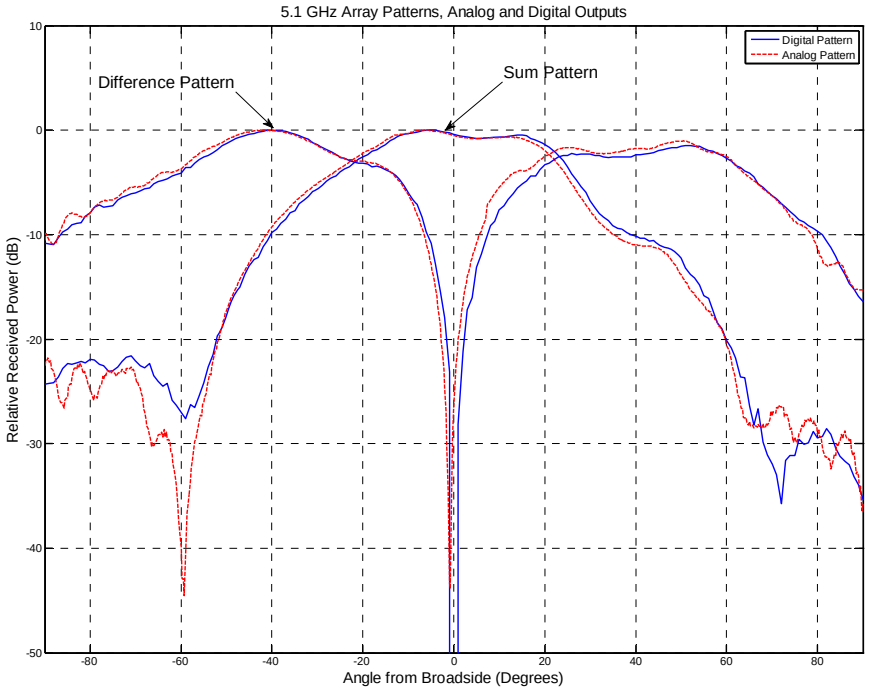

Figure 26: Direct comparison of analog vs. digital sum and difference patterns

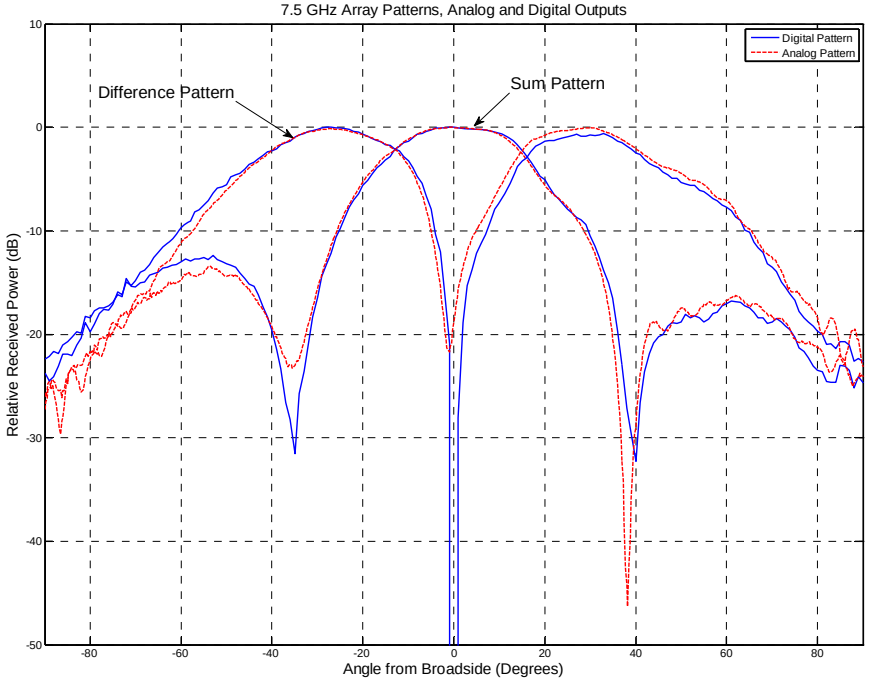

Figure 27: Direct comparison of analog vs. digital sum and difference patterns

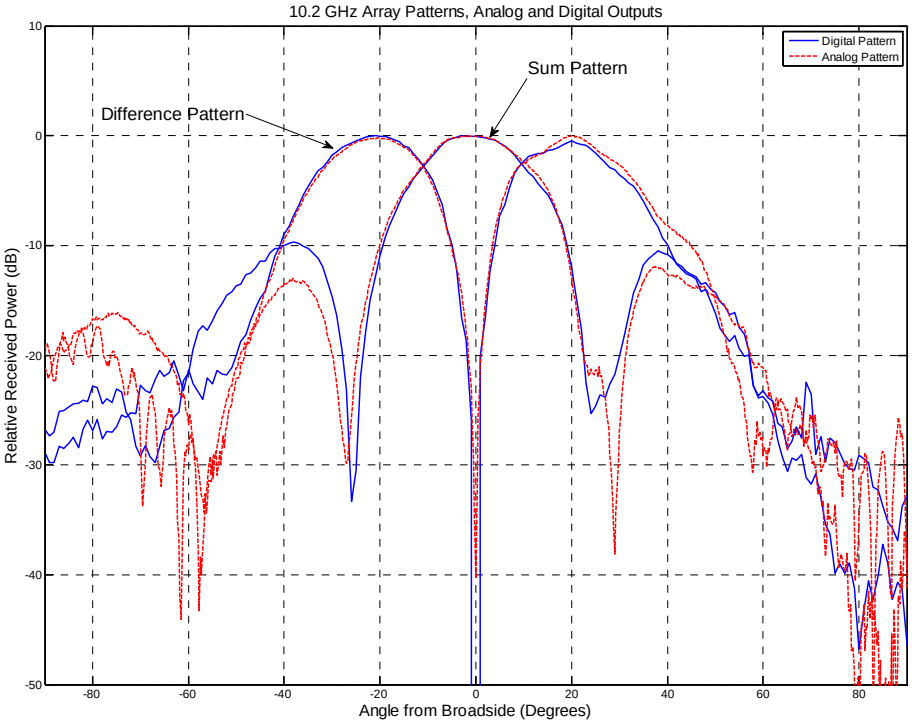

Figure 28: Direct comparison of analog vs. digital sum and difference patterns

6. Conclusions

A testbed system has been assembled that combines broadband phased arrays with multiple broadband digital receive channels. RF System Modeling, System Integration, and RF System Testing have been accomplished for this initial demonstration. Using data from the system, one can apply digital techniques to form digital antenna beams, as verified by comparison to analog antenna patterns.

The TELA testbed has been designed as an upgradeable system in order to assess current and future technologies at a system level. Future work planned includes the incorporation of broadband true time delay MMICs for analog calibration and beamsteering. The number of digital receiver channels will also be increased in order to increase the capability of the array. Future planned work also includes efforts to reduce the size and weight of the system while demonstrating even more advanced capabilities.

7. Acknowledgments

The authors wish to acknowledge the Dave Kuhl and the AFRL RASCAL facility for assistance in data collection.

8. References

[1] B. A. Munk et al., "A low-profile broadband phased array antenna," in *Proc. Antennas Propagation Soc. Int. Symposium*, Columbus, OH, Jun. 2003, pp. 448–451.

[2] L. Corey et al, "Phased-array Development at DARPA," *IEEE International Symposium on Phased Array Systems and Technology*, 14-17 Oct. 2003, pp. 9 – 16.

[3] R. Mongia et al., "Wideband Plastic Packaged Highly Integrated TR MMIC with Variable Time Delay," *GOMACTech-07 Proceedings*, March 2007.

[4] T. Quach et al., "X-Band Receiver Front-End Components in Silicon Technology," *GOMACTech-07 Proceedings*, March 2007.

[5] D. Spendley et al., "Initial demonstration of an X-band digital beamforming (DBF) receive array," *IEEE Aerospace Conference Proceedings*, March 2006.

[6] Pozar, David M., *Microwave Engineering, 3rd Edition*, Wiley, 2005.

[7] Syscalc Version 6.1.8, Arden Technologies Inc.

[8] Advanced Design System (ADS) 2006A, Agilent Technologies.

[9] Van Trees, Harry L., "Optimum Array Processing", John Wiley and Sons, Inc, New York, 2002.